Supporting Information for

Pd-Rh Nanocrystals with Tunable Morphologies and Compositions as Efficient Catalysts towards Suzuki Cross-coupling Reactions

Si-Bo Wang‡, Wei Zhu‡, Jun Ke, Mu Lin, Ya-Wen Zhang*

Beijing National Laboratory for Molecular Sciences, State Key Laboratory of Rare Earth Materials Chemistry and Applications, PKU-HKU Joint Laboratory in Rare Earth Materials and Bioinorganic Chemistry, College of Chemistry and Molecular Engineering, Peking University, Beijing 100871, China. Fax: +86-10-62756787; E-mail: ywzhang@pku.edu.cn.

‡ These authors contributed equally.

Experimental Section

Calculation of the total number of Pd atoms on the surface of Pd nanocubes (NCs), Pd-Rh hollow NCs, Pd-Rh nanoicosahedrons (NIs), Pd-Rh nanotruncated octahedrons (NTOs), Pd-Rh solid NCs, and commercial Pd/C.

(1) Pd NCs

The average edge length of Pd NCs is *ca.* 12 nm. Pd has face-centered-cubic structure with lattice constant of 0.389 nm and each unit cell contains four Pd atoms. So the total number of Pd atoms in one Pd NC is

$$TN_{\text{Pd NC}} = \frac{V_{\text{Pd NC}}}{V_{\text{cell}}} \times 4 = \frac{(12\ \text{nm})^3}{(0.389\ \text{nm})^3} \times 4 = 1.2 \times 10^5$$

A Pd NC is enclosed by six (100) facets, and each two-dimensional unit cell on the (100) facets contains two Pd atoms. The total number of Pd atoms on the surface of one Pd NC is

$$TNS_{\text{Pd NC}} = \frac{A_{\text{Pd NC}}}{A_{\text{cell}}} \times 2 = \frac{(12\ \text{nm})^2}{(0.389\ \text{nm})^2} \times 6 \times 2 = 1.1 \times 10^4$$

The total number of Pd atoms on the surface of Pd NCs used as catalyst is

$$m_{\text{Pd NC}} \times \frac{TNS_{\text{Pd NC}}}{TN_{\text{Pd NC}}} = \frac{50\ \mu\text{g} \times 6.02 \times 10^{23}\ \text{mol}^{-1}}{106.4\ \text{g} \cdot \text{mol}^{-1}} \times \frac{1.1 \times 10^4}{1.2 \times 10^5} = 2.6 \times 10^{16}$$

(2) Pd-Rh hollow NCs

The average edge length of $Pd_{0.32}Rh_{0.68}$ hollow NCs is *ca.* 14 nm, and the diameter of the hole inside the cube is *ca.* 8 nm. Both Pd and Rh have face-centered-cubic structure with lattice constants of 0.389 nm and 0.380 nm, respectively, and each unit cell contains four Pd or Rh atoms, respectively. The ICP result shows that the atom ratio of Pd and Rh is *ca.* 32:68, so the weighted average of the lattice constant for the Pd-Rh hollow NCs is 0.383 nm. Thus, the total number of metal atoms in one $Pd_{0.32}Rh_{0.68}$ hollow NC is

$$TN_{\text{Pd-Rh hollow NC}} = \frac{V_{\text{Pd-Rh hollow NC}}}{V_{\text{cell}}} \times 4 = \frac{(14\ \text{nm})^3 - (8\ \text{nm})^3}{(0.383\ \text{nm})^3} \times 4 = 1.6 \times 10^5$$

We assume that one $Pd_{0.32}Rh_{0.68}$ hollow NC is enclosed by six (100) facets, and each two-dimensional unit cell on the (100) facets contains two metal atoms. According to the XPS result, the atom ratio of Pd and Rh is *ca.* 24:76, so the weighted average of the lattice constant for the Pd-Rh hollow NC is 0.382 nm. The total number of Pd atoms on the surface of one NC is

$$TNS_{\text{Pd-Rh hollow NC}} = \frac{A_{\text{Pd-Rh hollow NC}}}{A_{\text{cell}}} \times 2 \times x_{Pd} = \frac{(14\ \text{nm})^2 + (8\ \text{nm})^2}{(0.382\ \text{nm})^2} \times 6 \times 2 \times 0.24 = 5.1 \times 10^3$$

The total number of Pd atoms on the surface of $Pd_{0.32}Rh_{0.68}$ hollow NCs used as catalyst is

$$m_{\text{Pd-Rh hollow NC}} \times \frac{TNS_{\text{Pd-Rh hollow NC}}}{TN_{\text{Pd-Rh hollow NC}}} = \frac{50\ \mu\text{g} \times 6.02 \times 10^{23}\ \text{mol}^{-1}}{106.4\ \text{g} \cdot \text{mol}^{-1} \times 0.32 + 104.9\ \text{g} \cdot \text{mol}^{-1} \times 0.68} \times \frac{5.1 \times 10^{3}}{1.6 \times 10^{5}} = 9.1 \times 10^{15}$$

According to the procedure above and ICP as well as XPS results (Table S2 and S3), total number of Pd atoms on the surface of $Pd_{0.68}Rh_{0.32}$, $Pd_{0.49}Rh_{0.51}$, and $Pd_{0.22}Rh_{0.78}$ hollow NCs is 2.3×10^{16}, 1.5×10^{16} and 5.7×10^{15}, respectively.

Additionally, given that the relative atomic masses and lattice constants of Pd and Rh are similar, relative error of total number of Pd atoms on the surface of Pd-Rh hollow NCs used as catalyst we calculated is less than 2%.

(3) Pd-Rh NIs

The average diameter of Pd-Rh NIs is *ca.* 16 nm. Both Pd and Rh have face-centered-cubic structure with lattice constants of 0.389 nm and 0.380 nm, respectively, and each unit cell contains four Pd or Rh atoms, respectively. The ICP result shows that the atom ratio of Pd and Rh is *ca.* 68:32, so the weighted average of the lattice constant for the Pd-Rh NIs is 0.386 nm. Thus, the total number of metal atoms in a single Pd-Rh NI is

$$TN_{\text{Pd-Rh NI}} = \frac{V_{\text{Pd-Rh NI}}}{V_{\text{cell}}} \times 4 = \frac{\frac{15+5\sqrt{5}}{12} \times \left(\sqrt{\frac{10-2\sqrt{5}}{5}} \times \frac{16\ \text{nm}}{2}\right)^{3}}{(0.386\ \text{nm})^{3}} \times 4 = 9.0 \times 10^{4}$$

We assume that a Pd-Rh NI is enclosed by twenty (111) facets and each two-dimensional unit cell on the (111) facets contains two metal atoms. According to the XPS result, the atom ratio of Pd and Rh is *ca.* 60:40, so the weighted average of the lattice constant for the Pd-Rh NIs is 0.385 nm. The total number of Pd atoms on the surface of one NI is

$$TNS_{\text{Pd-Rh NI}} = \frac{A_{\text{Pd-Rh NI}}}{A_{\text{cell}}} \times 2 \times x_{Pd} = \frac{\frac{\sqrt{3}}{4} \times \left(\frac{16\ \text{nm}}{2}\right)^{2} \times \frac{10-2\sqrt{5}}{5}}{\frac{\sqrt{3}}{4} \times \left(\sqrt{2} \times 0.385\ \text{nm}\right)^{2}} \times 20 \times 2 \times 0.60 = 5.7 \times 10^{3}$$

The total number of Pd atoms on the surface of Pd-Rh NIs used as catalyst is

$$m_{\text{Pd-Rh NI}} \times \frac{TNS_{\text{Pd-Rh NI}}}{TN_{\text{Pd-Rh NI}}} = \frac{50\ \mu\text{g} \times 6.02 \times 10^{23}\ \text{mol}^{-1}}{106.4\ \text{g} \cdot \text{mol}^{-1} \times 0.68 + 104.9\ \text{g} \cdot \text{mol}^{-1} \times 0.32} \times \frac{5.7 \times 10^{3}}{9.0 \times 10^{4}} = 1.8 \times 10^{16}$$

Additionally, given that the relative atomic masses and lattice constants of Pd and Rh are similar, relative error of total number of Pd atoms on the surface of Pd-Rh NIs used as catalyst we calculated is less than 2%.

(4) Pd-Rh NTOs

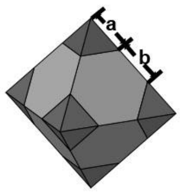

The average diameter of Pd-Rh NTOs is *ca.* 12 nm. And according to the geometric model above, the relationship of edge length and diameter of a NTO is

$$5a^{2} + 3b^{2} + 6ab = (12\,\text{nm})^{2}$$

Both Pd and Rh have face-centered-cubic structure with lattice constants of 0.389 nm and 0.380 nm, respectively, and each unit cell contains four Pd or Rh atoms, respectively. The ICP result shows that the atom ratio of Pd and Rh is *ca.* 67:33, so the weighted average of the lattice constant for the Pd-Rh NTOs is 0.386 nm. Thus, the total number of metal atoms in a single Pd-Rh truncated octahedron is

$$TN_{\text{Pd-Rh NTO}} = \frac{V_{\text{Pd-Rh NTO}}}{V_{\text{cell}}} \times 4 = \frac{\frac{\sqrt{2}}{3}(b+2a)^3 - 3\times\frac{\sqrt{2}}{3}a^3}{(0.386\ \text{nm})^2} \times 4$$

We assume that a Pd-Rh NTO is enclosed by six (100) facets and eight (111) facets, and each two-dimensional unit cell on the (100) or (111) facets contains two metal atoms. According to the XPS result, the atom ratio of Pd and Rh is *ca.* 61:39, so the weighted average of the lattice constant for the Pd-Rh NTOs is 0.385 nm. The total number of Pd atoms on the surface of one NTO is

$$TNS_{\text{Pd-Rh NTO}} = \frac{A_{\text{Pd-Rh NTO}}}{A_{\text{cell}}} \times 2 \times x_{Pd} = \left(\frac{6a^2}{(0.385\ \text{nm})^2} + \frac{2\sqrt{3}b^2 + 8\sqrt{3}ab + 2\sqrt{3}a^2}{\frac{\sqrt{3}}{4}\times\left(\sqrt{2}\times 0.385\ \text{nm}\right)^2} \right) \times 2 \times 0.61$$

The total number of Pd atoms on the surface of Pd-Rh NTOs used as catalyst is

$$m_{\text{Pd-Rh NTO}} \times \frac{TNS_{\text{Pd-Rh NTO}}}{TN_{\text{Pd-Rh NTO}}} = \frac{50\ \mu\text{g} \times 6.02\times10^{23}\ \text{mol}^{-1}}{106.4\ \text{g}\cdot\text{mol}^{-1}\times 0.67 + 104.9\ \text{g}\cdot\text{mol}^{-1}\times 0.33} \times \frac{TN_{\text{Pd-Rh NTO}}}{TNS_{\text{Pd-Rh NTO}}}$$

According to the HRTEM images of NTOs (Figure 2g), the average length of *a* is ca. 3.7 nm. And we calculated the total number of Pd atoms with different *a* (the maximum of *a* is around 5.3 nm due to geometrical issues, Table S4), suggesting the mere change of it when *a* changed in the range of 3.3 nm to 4.3 nm. Thus, we assume the total number of Pd atoms is 2.7×10^{16}.

Additionally, given that the relative atomic masses and lattice constants of Pd and Rh are similar, relative error of total number of Pd atoms on the surface of Pd-Rh NIs used as catalyst we calculated is less than 2%.

(5) Pd-Rh solid NCs

The average edge length of a Pd-Rh solid NCs is *ca.* 9 nm. Both Pd and Rh have face-centered-cubic structure with lattice constants of 0.389 nm and 0.380 nm, respectively, and each unit cell contains four Pd or Rh atoms, respectively. The ICP result shows that the atom ratio of Pd and Rh is *ca.* 69:31, so the weighted average of the lattice constant for the Pd-Rh solid NCs is *ca.* 0.386 nm. Thus, the total number of metal atoms in a single Pd-Rh solid NC is

$$TN_{\text{Pd-Rh NC}} = \frac{V_{\text{Pd-Rh NC}}}{V_{\text{cell}}} \times 4 = \frac{(9\ \text{nm})^3}{(0.386\ \text{nm})^3} \times 4 = 5.1\times10^4$$

We assume that a Pd-Rh solid NC is enclosed by six (100) facets and each two-dimensional unit cell on the (100) facets contains two metal atoms. According to the XPS result, the atom ratio of Pd and Rh is *ca.* 62:38, so the weighted average of the lattice constant for the Pd-Rh solid NCs is 0.386 nm. The total number of Pd atoms on the surface of one NC is

$$TNS_{\text{Pd-Rh NC}} = \frac{A_{\text{Pd-Rh NC}}}{A_{\text{cell}}} \times 2 \times x_{Pd} = \frac{(9\ \text{nm})^2}{(0.386\ \text{nm})^2} \times 6 \times 2 \times 0.62 = 4.0\times10^3$$

The total number of Pd atoms on the surface of Pd-Rh solid NCs used as catalyst is

$$m_{\text{Pd-Rh NC}} \times \frac{TNS_{\text{Pd-Rh NC}}}{TN_{\text{Pd-Rh NC}}} = \frac{50\ \mu\text{g} \times 6.02\times10^{23}\ \text{mol}^{-1}}{106.4\ \text{g}\cdot\text{mol}^{-1}\times 0.69 + 104.9\ \text{g}\cdot\text{mol}^{-1}\times 0.31} \times \frac{4.0\times10^3}{5.1\times10^4} = 2.2\times10^{16}$$

Additionally, given that the relative atomic masses and lattice constants of Pd and Rh are similar, relative error of total number of Pd atoms on the surface of Pd-Rh solid NCs used as catalyst we calculated is less than 2%.

(6) Commercial Pd/C

The average diameter of a Pd NP is *ca.* 6 nm. Pd has face-centered-cubic structure with lattice constant of 0.389 nm and each unit cell contains four Pd atoms. So the total number of Pd atoms in a single Pd/C NP is

$$TN_{\text{Pd/C}} = \frac{V_{\text{Pd/C}}}{V_{\text{cell}}} \times 4 = \frac{4}{3}\pi \times \frac{(\frac{6\ \text{nm}}{2})^3}{(0.389\ \text{nm})^3} \times 4 = 7.7\times10^3$$

We assume that (a) a Pd NP is enclosed by (100) facets and each two-dimensional unit cell on the (100) facets contains two Pd atoms. The total number of Pd atoms on the surface of one Pd nanoparticle is

$$TNS_{\text{Pd/C}} = \frac{A_{\text{Pd/C}}}{A_{\text{cell}}} \times 2 = \frac{4\pi \times (\frac{6\text{ nm}}{2})^2}{(0.389\text{ nm})^2} \times 2 = 1.5 \times 10^3$$

(b) a Pd NP is enclosed by (111) facets and each two-dimensional unit cell on the (111) facets contains two Pd atoms. The total number of Pd atoms on the surface of one Pd nanoparticle is

$$TNS_{\text{Pd/C}} = \frac{A_{\text{Pd/C}}}{A_{\text{cell}}} \times 2 = \frac{4\pi \times (\frac{6\text{ nm}}{2})^2}{\frac{\sqrt{3}}{4} \times \left(\sqrt{2} \times 0.385\text{ nm}\right)^2} \times 2 = 1.7 \times 10^3$$

Thus, there is no big difference between two assumptions. So we assume that the total number of Pd atoms on the surface of one Pd nanoparticle is 1.6×10^3.

The total number of Pd atoms on the surface of Pd nanoparticles used as catalyst is

$$m_{\text{Pd/C}} \times \frac{TNS_{\text{Pd/C}}}{TN_{\text{Pd/C}}} = \frac{50\ \mu\text{g} \times 6.02 \times 10^{23}\ \text{mol}^{-1}}{106.4\ \text{g} \cdot \text{mol}^{-1}} \times \frac{1.6 \times 10^3}{7.7 \times 10^3} = 5.9 \times 10^{16}$$

Supplementary Data

Table S1. ICP-AES results of Pd/Rh ratios in Pd-Rh hollow NCs synthesized at different temperatures.

Temperature / ˚C	Atomic ratio in Pd-Rh hollow NCs
140	60:40
160	33:67
180	32:68
200	30:70

Table S2. ICP-AES results of Pd/Rh ratios in Pd-Rh hollow NCs with reference to those in metal precursors.

Atomic ratio in precursors	Atomic ratio in Pd-Rh hollow NCs
2:1	68:32
1:1	49:51
1:2	32:68
1:3	28:72
1:4	22:78
1:5	16:84
1:10	9:91

Table S3. XPS results of Pd/Rh ratios on the surface of Pd-Rh hollow NCs with reference to those in metal precursors.

Atomic ratio in precursors	Atomic ratio on the surface of Pd-Rh hollow NCs
2:1	61:39
1:1	40:60
1:2	24:79
1:4	15:85

Table S4. The total number of Pd atoms on the surface of Pd-Rh NTOs calculated with various *a*.

a / nm	The total number of Pd atoms
2.3	3.0×10^{16}
3.3	2.8×10^{16}
4.3	2.6×10^{16}
5.3	2.6×10^{16}

Table S5. XPS results of Pd(0):Pd(II) and Rh(0):Rh(III) of Pd-Rh nanocrystals in different shapes.

	Pd(0):Pd(II)	Rh(0):Rh(III)
Hollow NCs	64:36	63:37
Solid NCs	68:32	62:38
NIs	67:33	66:34
NTOs	64:36	67:33

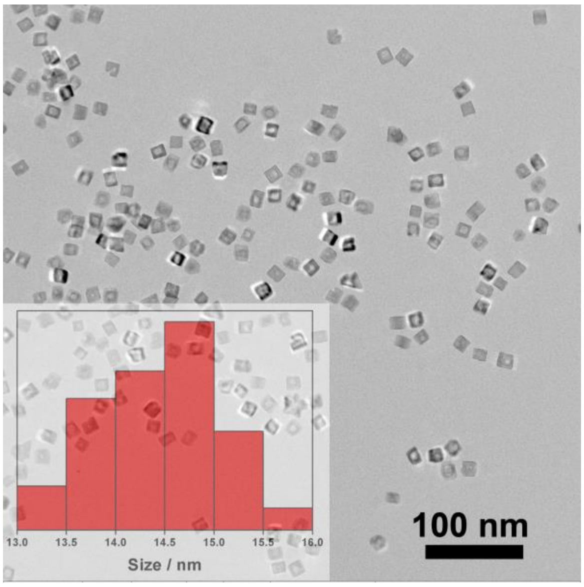

Figure S1. Low-magnification TEM image of Pd-Rh hollow NCs (the inset is the size distribution of Pd-Rh hollow NCs).

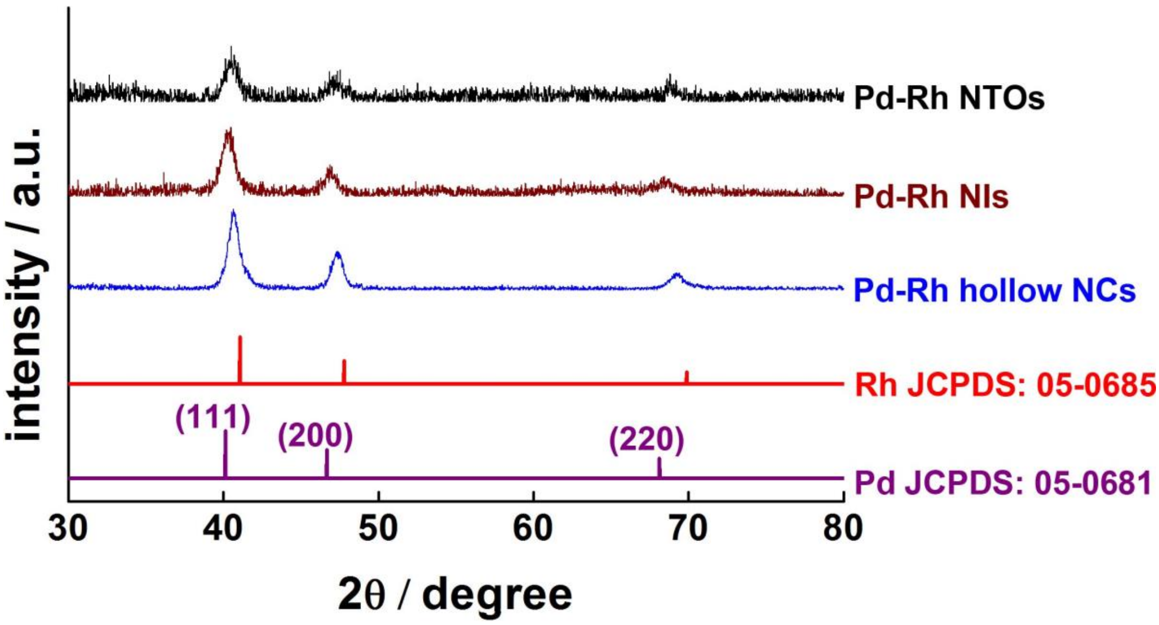

Figure S2. PXRD patterns of Pd-Rh hollow NCs, Pd-Rh NIs, and Pd-Rh NTOs with standard XRD data as references.

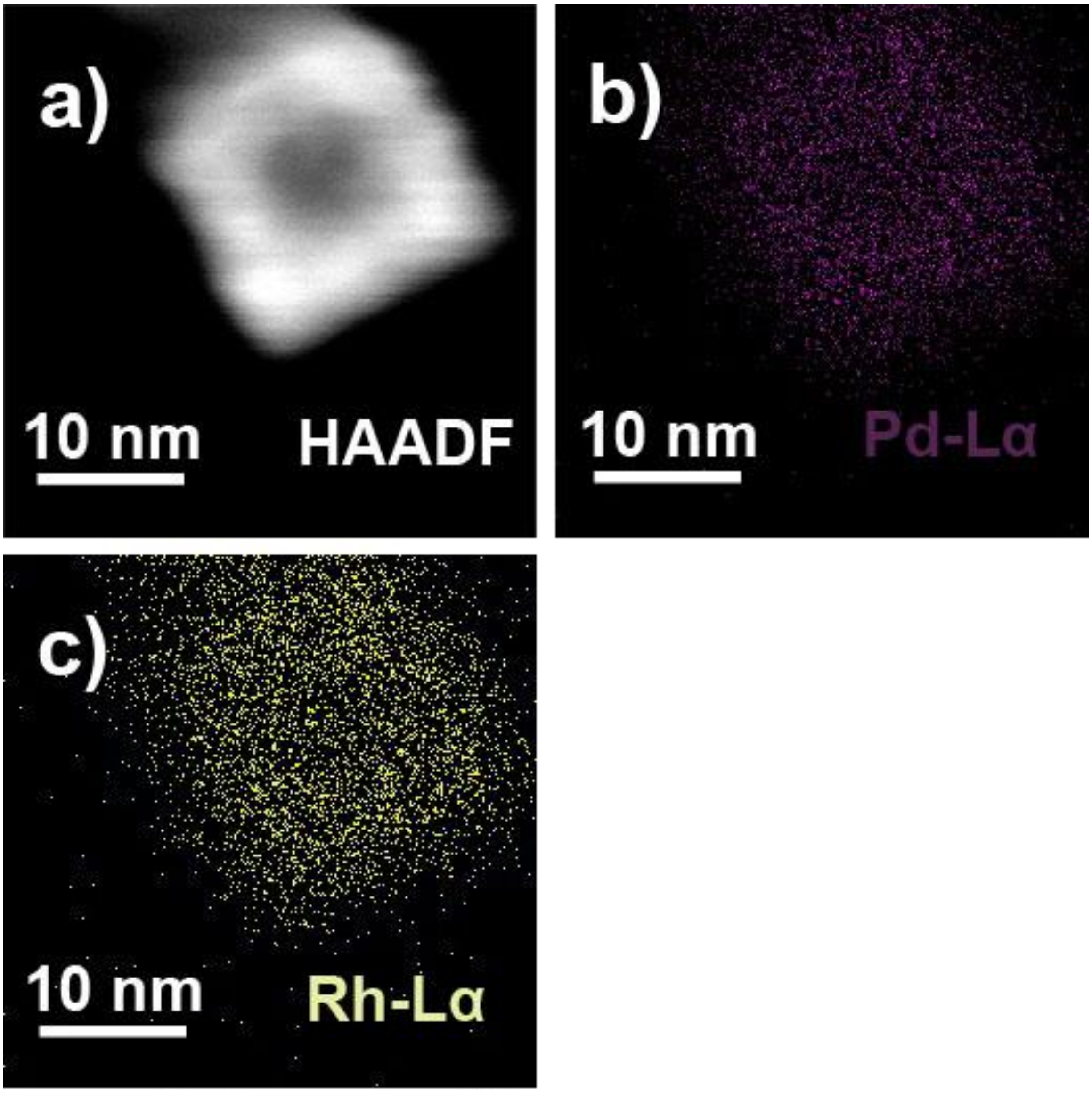

Figure S3. HAADF-STEM image and HAADF-STEM-EDS element maps of Pd-Rh hollow NCs: a) HAADF-STEM image, b) Pd contribution, and c) Rh contribution.

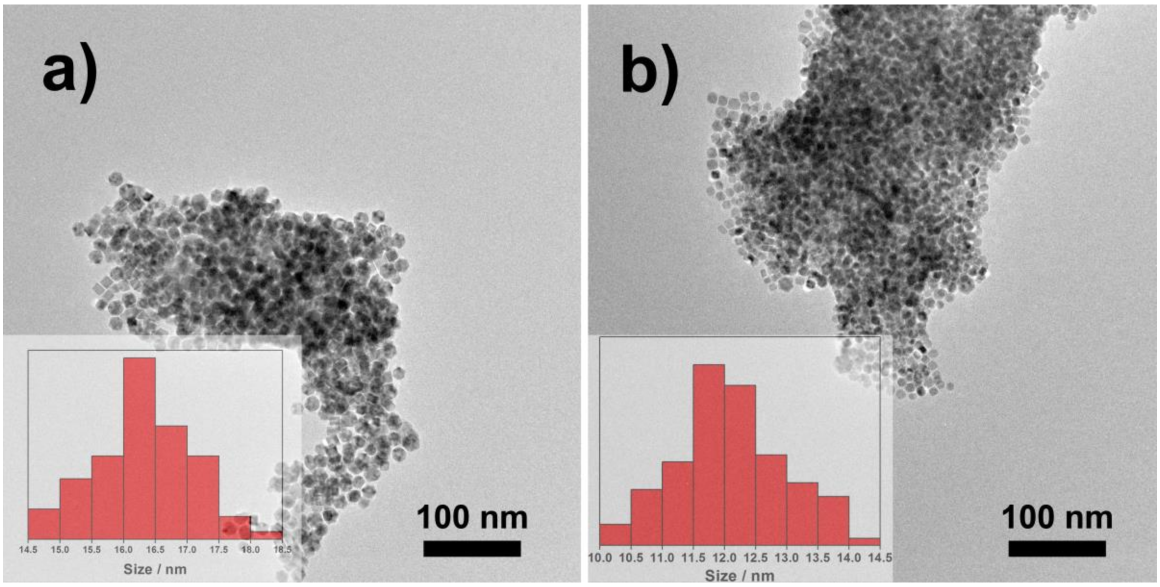

Figure S4. Low-magnification TEM images of a) Pd-Rh NIs, and b) Pd-Rh NTOs (insets are size distributions of Pd-Rh NIs and NTOs, respectively).

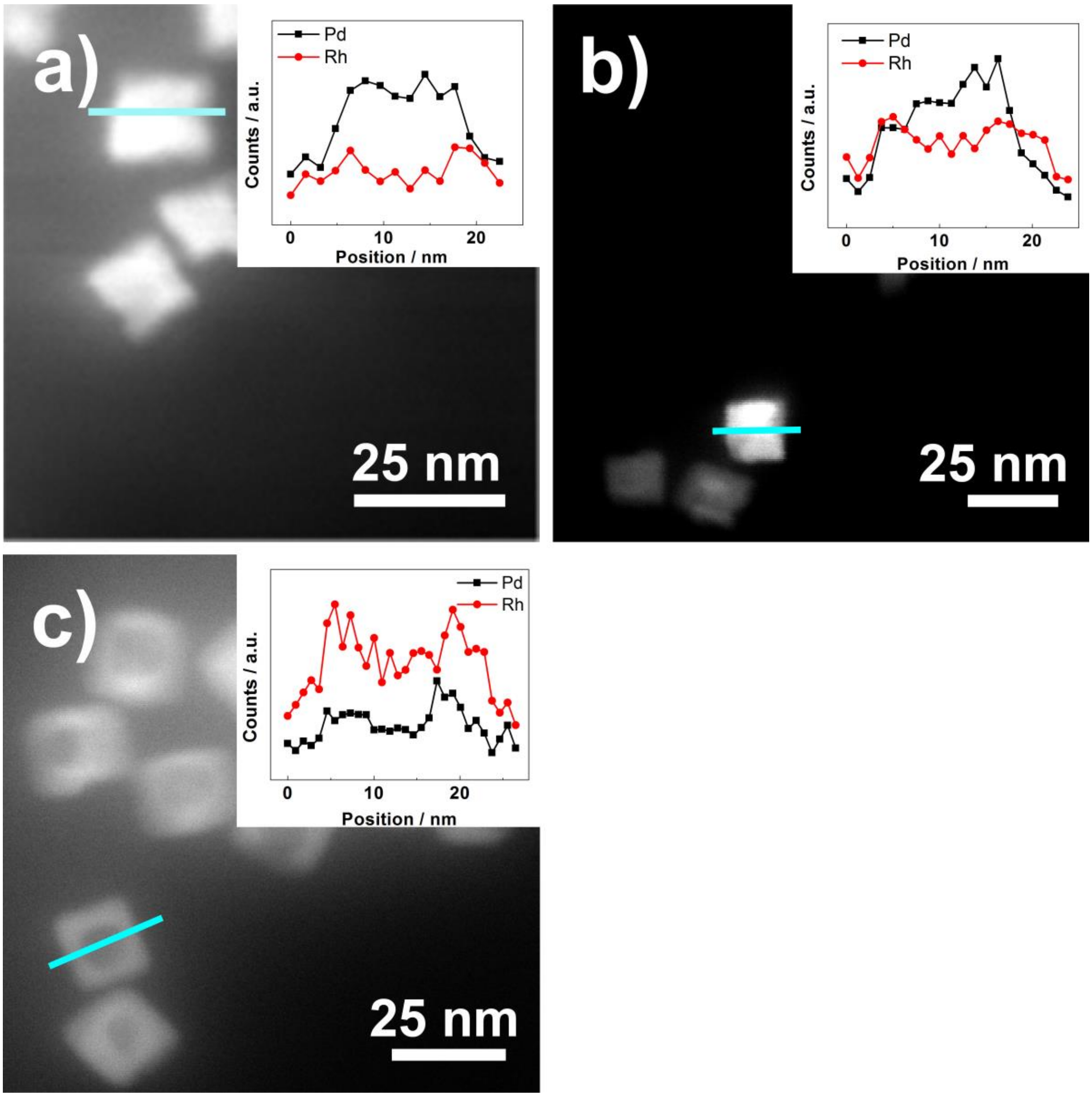

Figure S5. HAADF-STEM-EDS line-scan profiles of Pd-Rh hollow NCs taken at different stages during synthesis: a) 1 h, b) 2 h, and c) 24 h.

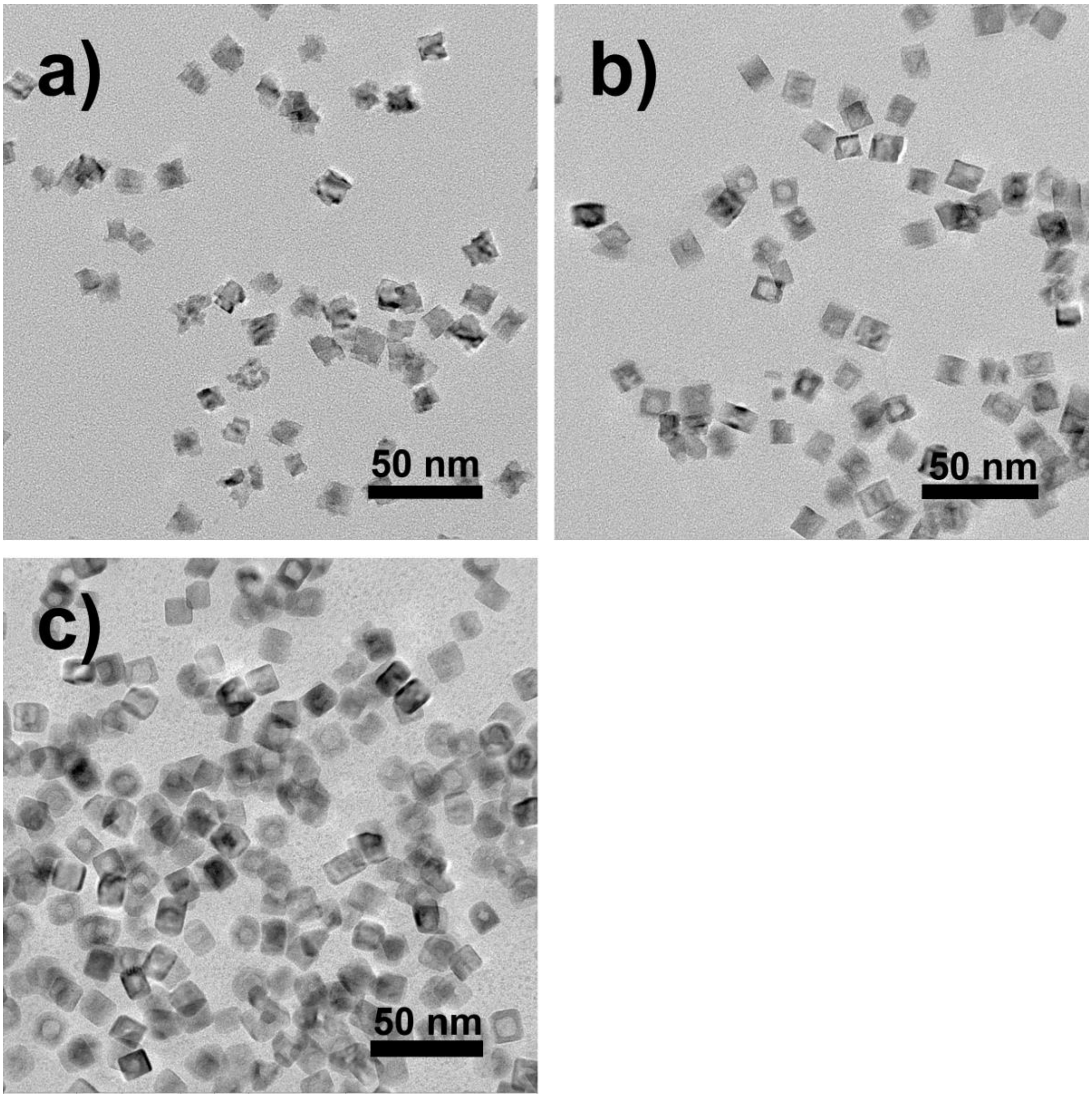

Figure S6. TEM images of Pd-Rh hollow NCs synthesized at different temperatures: a) 140 ˚C, b) 160 ˚C, and c) 200 ˚C.

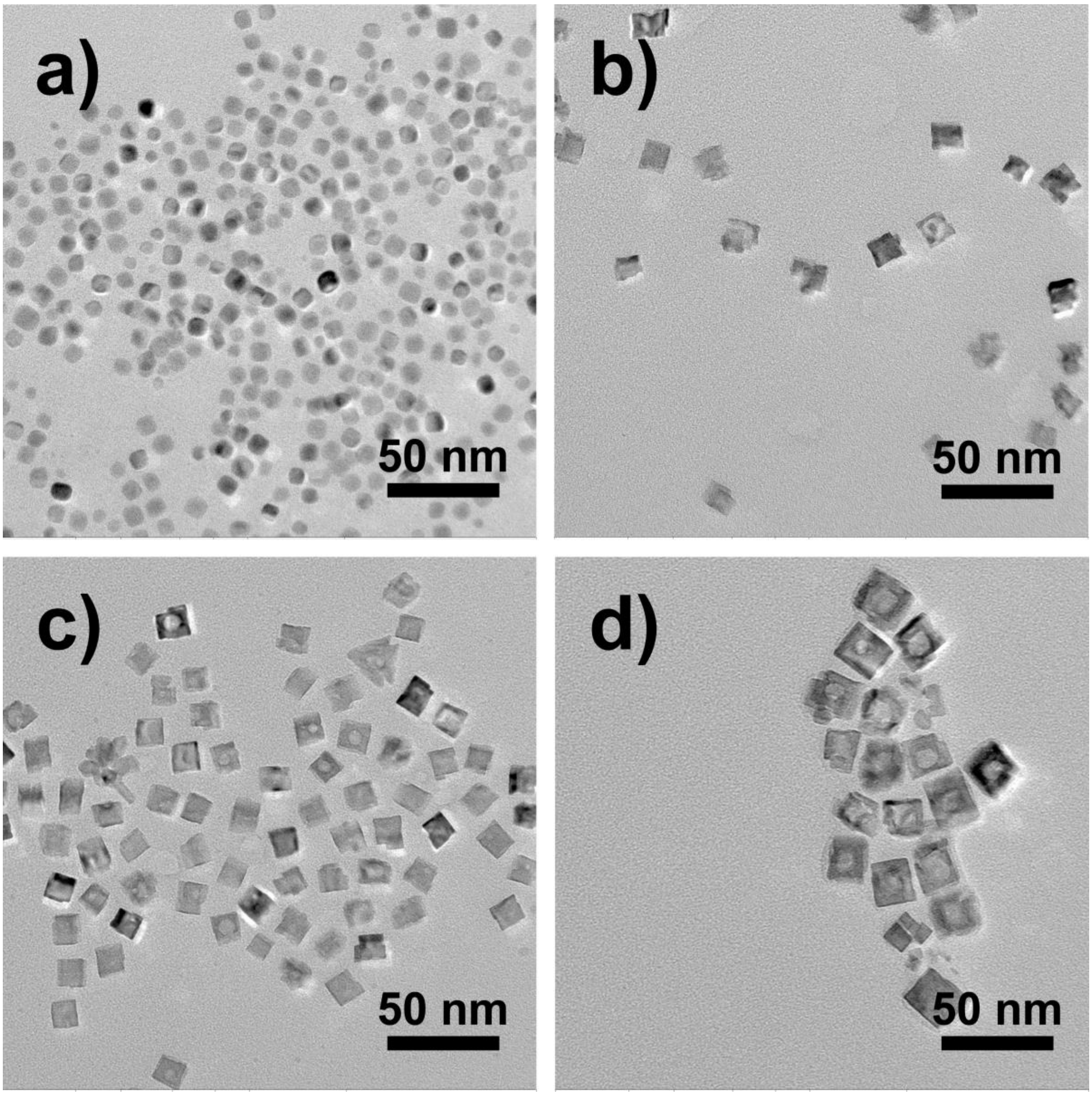

Figure S7. TEM images of Pd-Rh hollow NCs synthesized at 140 ˚C taken at various reaction times: a) 1 h, b) 6 h, c) 8 h, and d) 24 h.

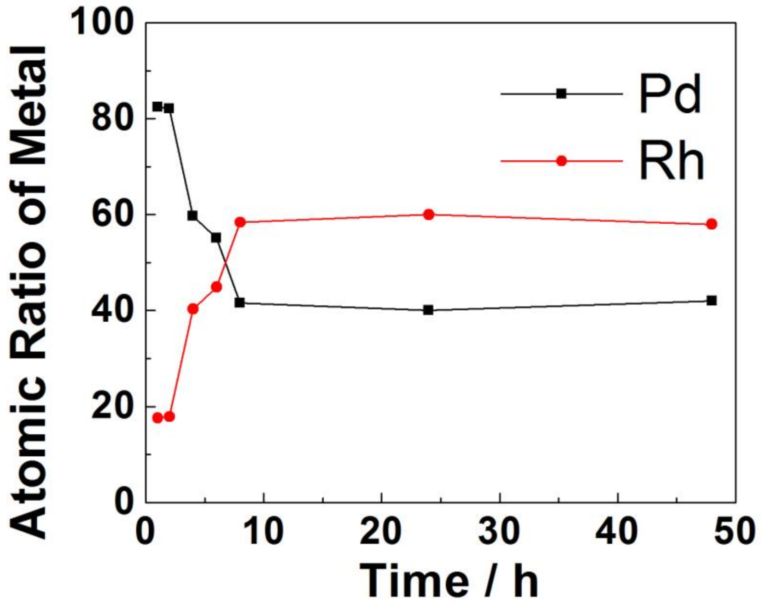

Figure S8. Atomic ratios (ICP-AES results) of Pd and Rh in Pd-Rh hollow NCs synthesized at 140 ˚C taken at different stages during synthesis.

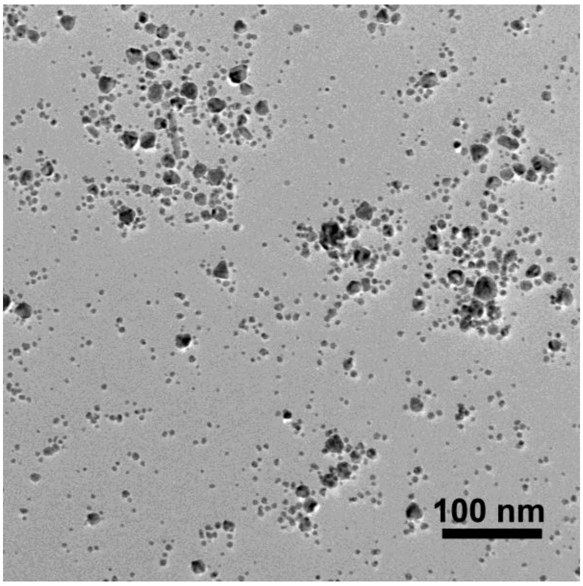

Figure S9. TEM image of Pd-Rh nanoparticles synthesized without KBr or KI added. All the other conditions were the same as those of Pd-Rh hollow NCs.

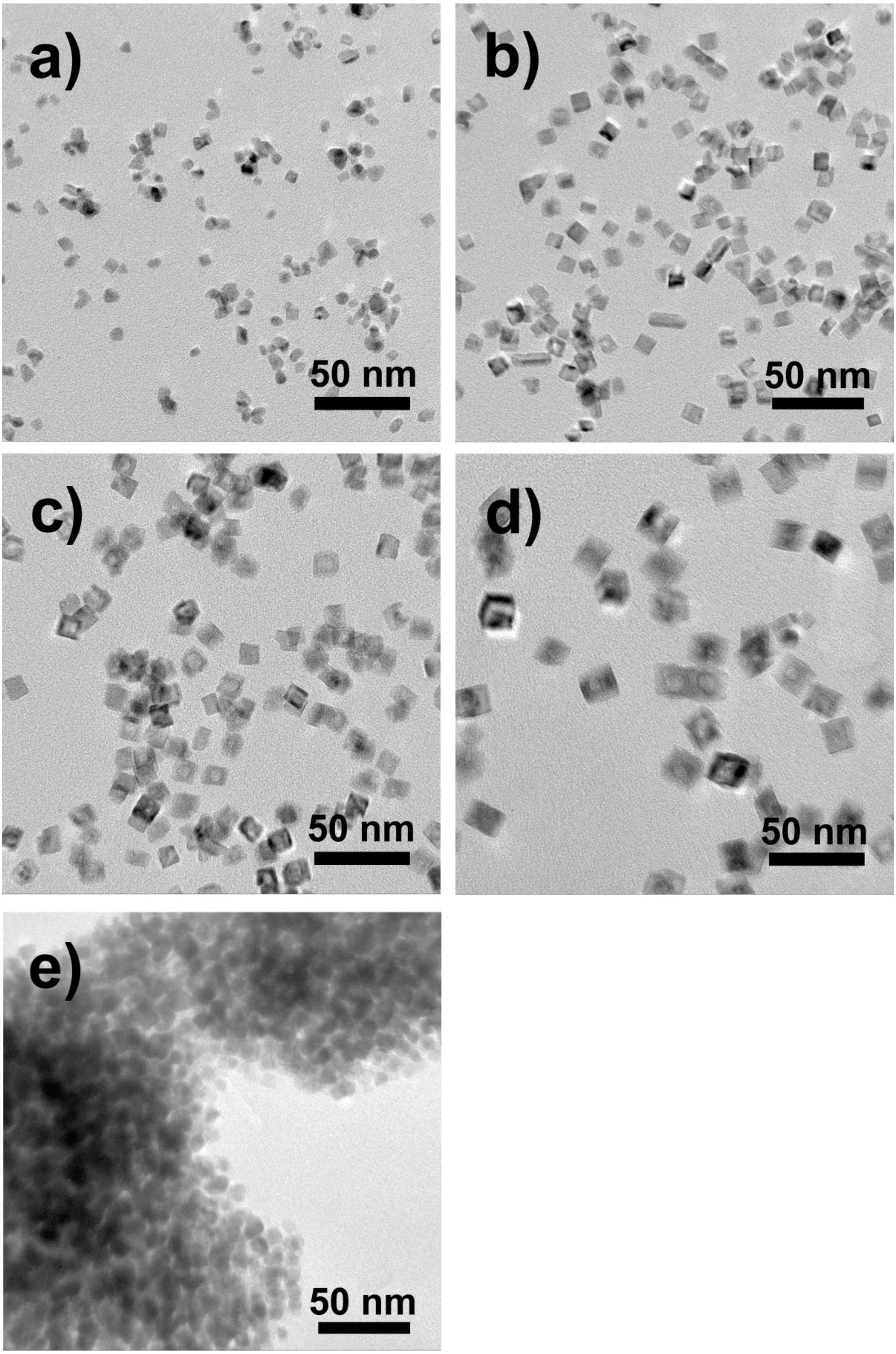

Figure S10. TEM images of Pd-Rh hollow NCs synthesized with different amounts of KBr: a) 0 mg, b) 180 mg, c) 360 mg, d) 1440 mg, and e) 2880 mg. All the other conditions were the same as those of Pd-Rh hollow NCs.

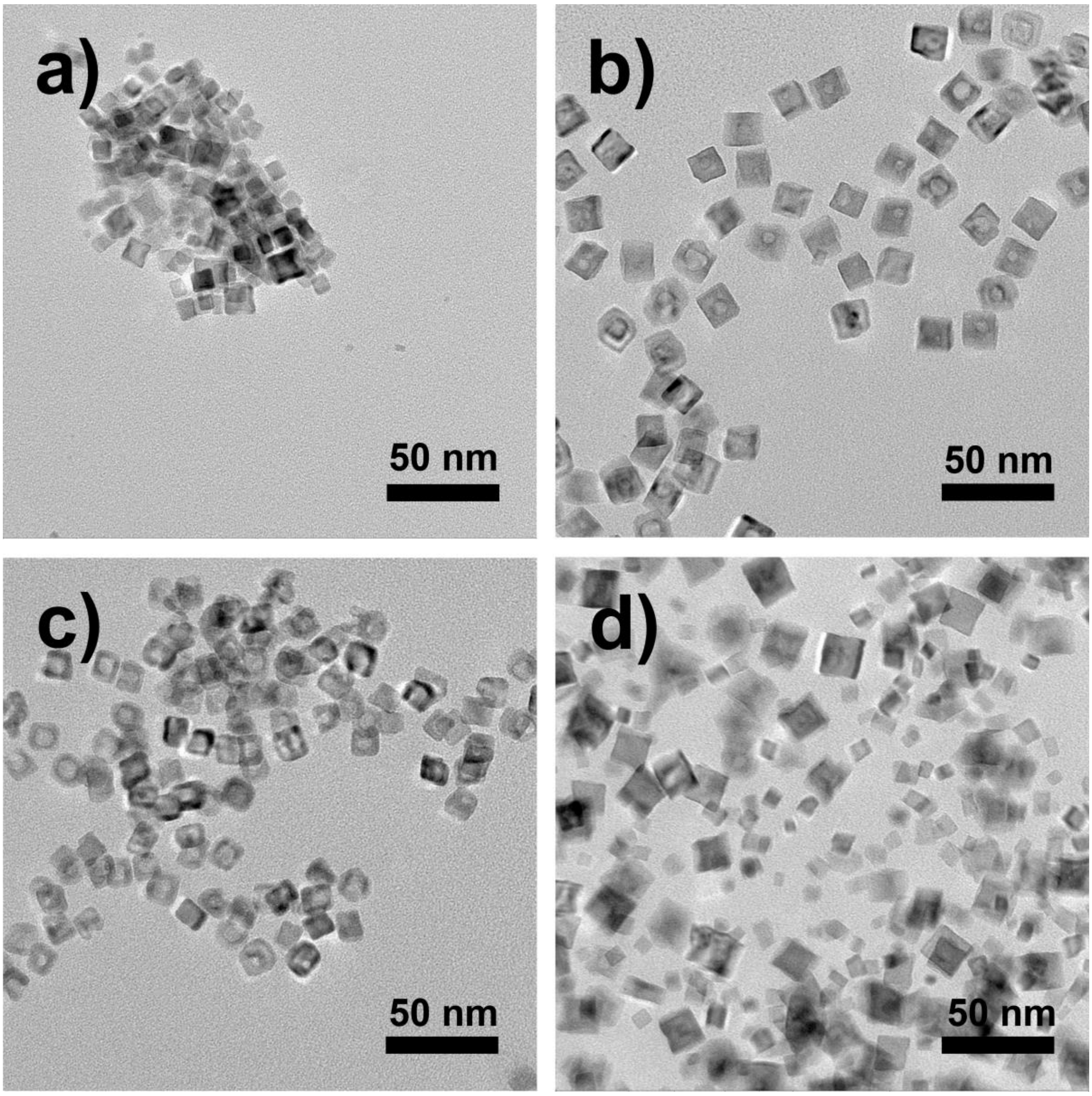

Figure S11. TEM images of Pd-Rh hollow NCs synthesized with different amounts of KI: a) 0 mg, b) 0.5 mg, c) 2 mg, and d) 4 mg. All the other conditions were the same as those of Pd-Rh hollow NCs.

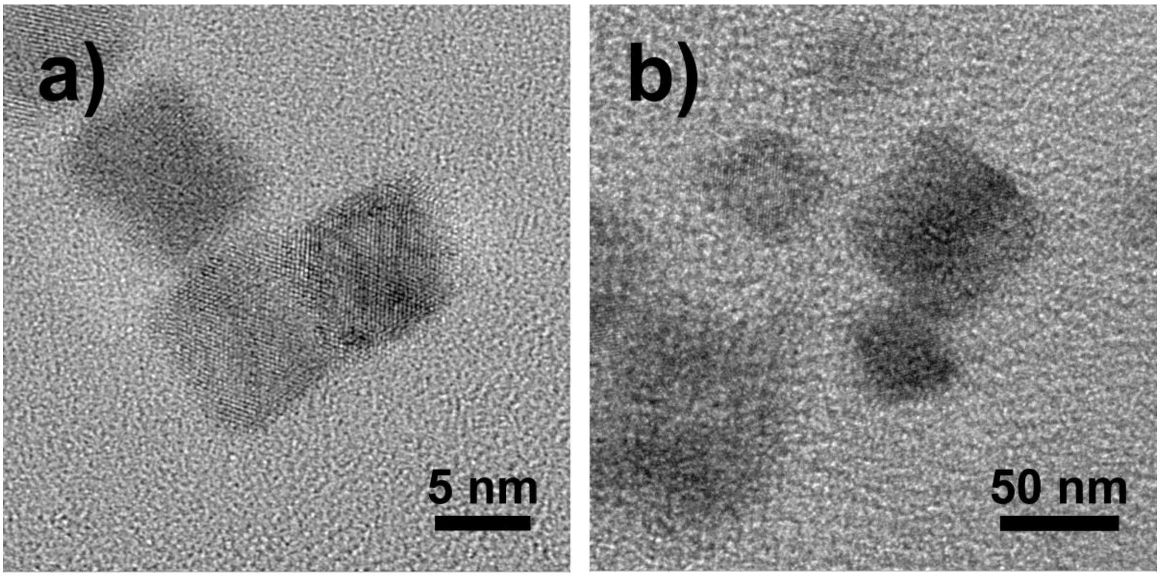

Figure S12. HRTEM images of solid $Pd_{0.32}Rh_{0.68}$ solid NCs a) before and b) after hydrothermal etching treatment. The Pd/Rh ratio in the NCs decreased from 33:67 to 29:71 after the etching process, indicating that a portion of Pd atoms were etched out from the interiors of the NCs, along with that the surfaces of the NCs became rough and porous.

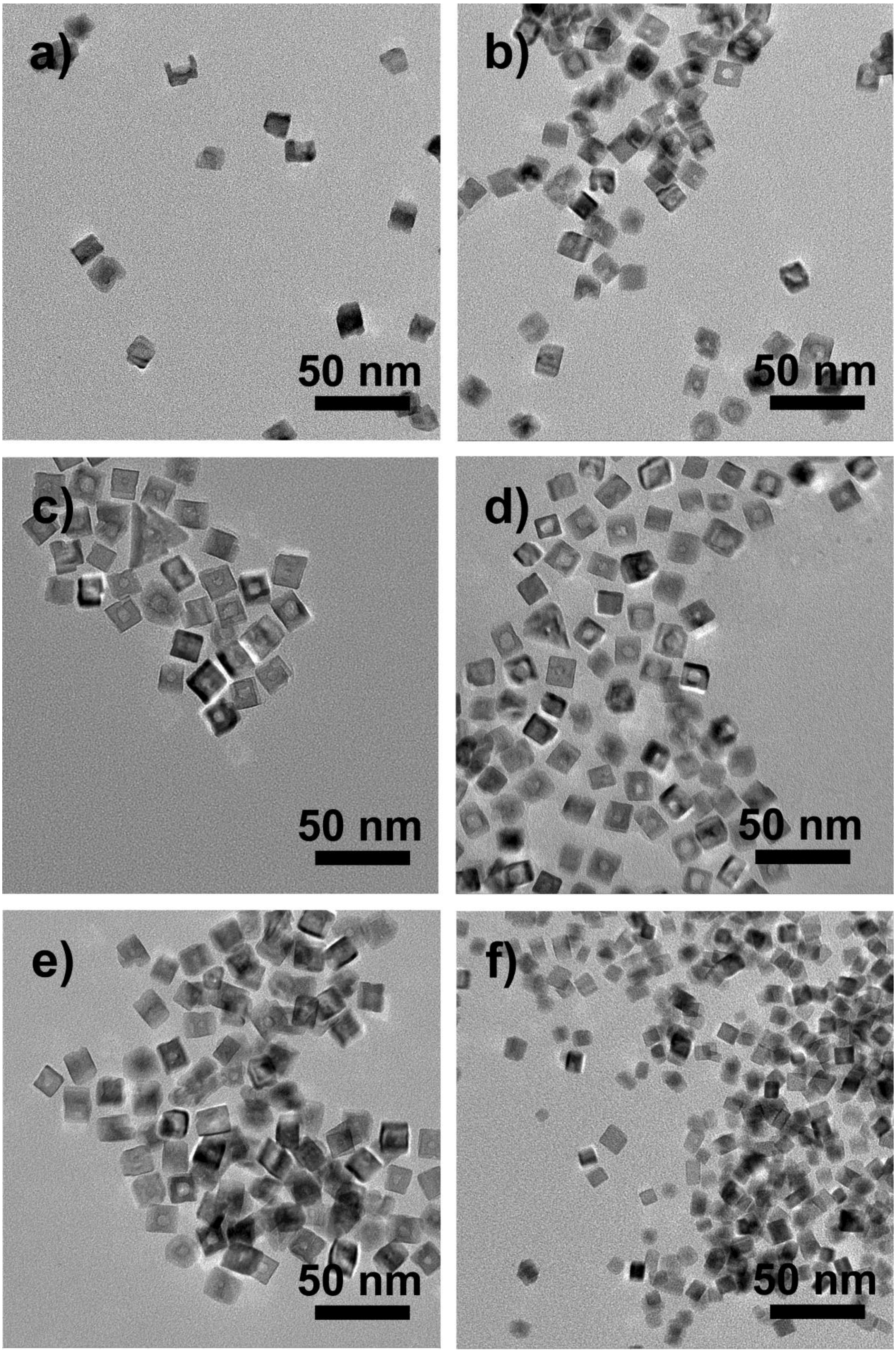

Figure S13. TEM images of Pd-Rh hollow NCs synthesized with different molar ratios of noble metal precursors at 180 °C for 4 h: a) Pd : Rh = 2 : 1; b) Pd: Rh = 1 : 1; c) Pd : Rh = 1 : 3, d) Pd : Rh = 1 : 5, e) Pd : Rh = 1 : 10, and f) 100% Rh (without addition of Na_2PdCl_4). The absolute moles of noble metal precursors were kept the same in all syntheses above. And all the other conditions were the same as those of Pd-Rh hollow NCs. Additionally, all those hollow NCs held the same proportion of palladium and rhodium as the corresponding precursors (Table S2).

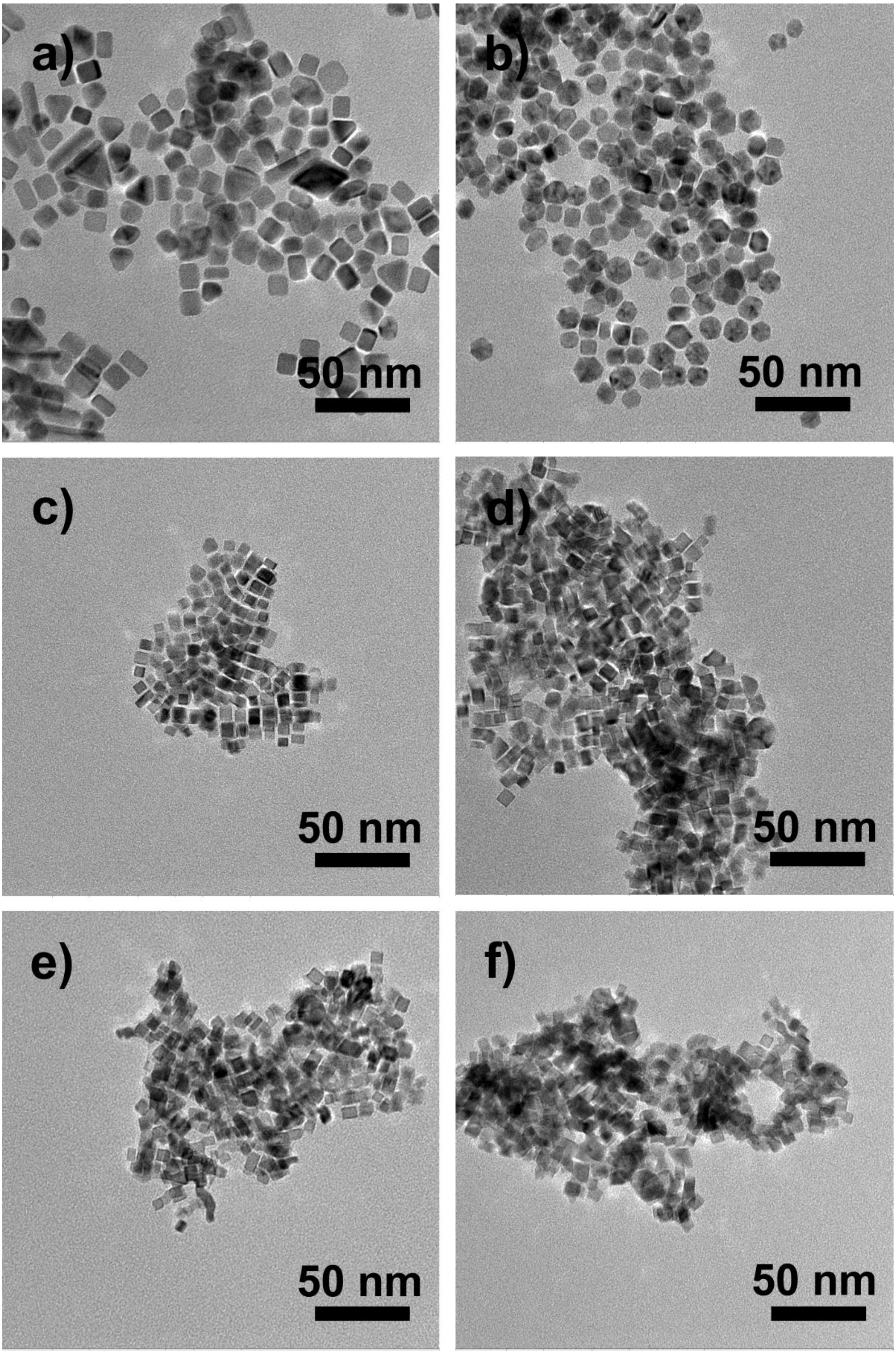

Figure S14. TEM images of Pd-Rh NIs synthesized with different molar ratios of noble metal precursors at 180 °C for 4 h: a) 100% Pd (without addition of $RhCl_3$), b) Pd : Rh = 5 : 1; c) Pd: Rh = 1 : 1; d) Pd : Rh = 1 : 2, e) Pd : Rh = 1 : 5, and f) 100% Rh (without addition of Na_2PdCl_4). The absolute moles of noble metal precursors were kept the same in all syntheses above. And all the other conditions were the same as those of Pd-Rh NIs.

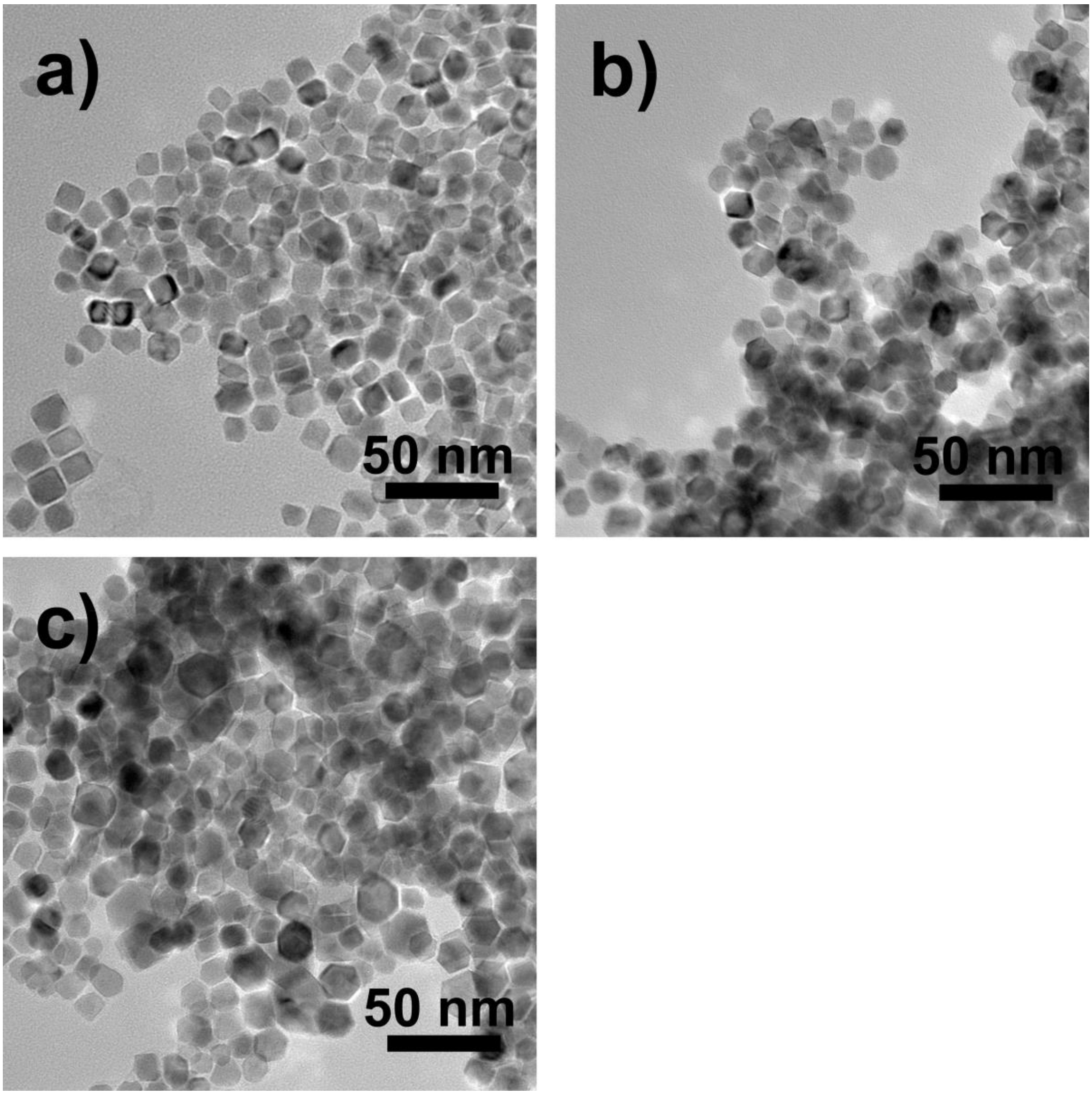

Figure S15. TEM images of Pd-Rh NTOs taken at various reaction times: a) 2 h, b) 8 h, and c) 24 h.

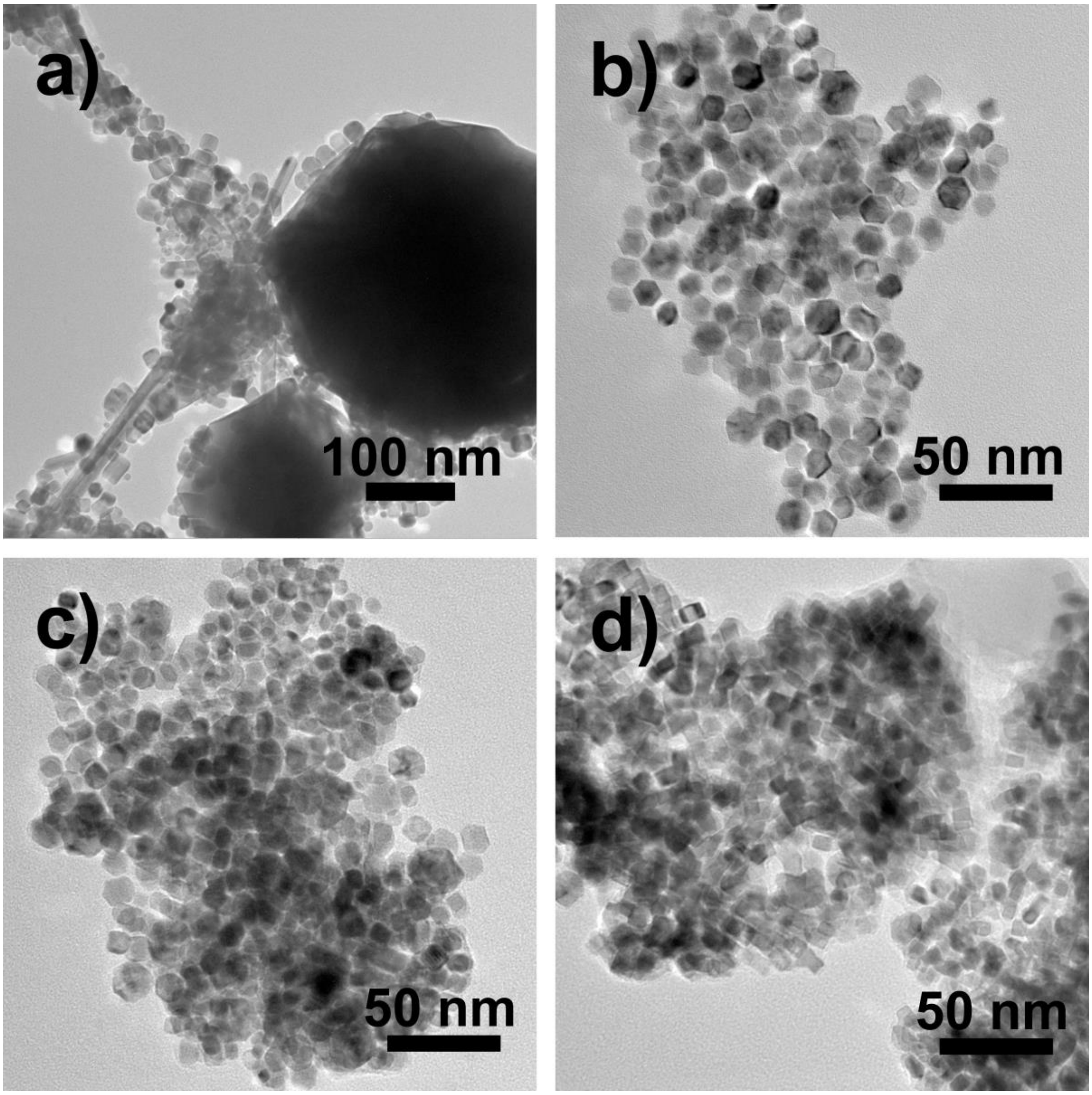

Figure S16. TEM images of Pd-Rh NTOs synthesized with different molar ratios of noble metal precursors at 180 °C for 4 h: a) 100% Pd (without addition of $RhCl_3$), b) Pd: Rh = 1 : 1; c) Pd : Rh = 1 : 2, and d) 100% Rh (without addition of Na_2PdCl_4). The absolute moles of noble metal precursors were kept the same in all syntheses above. And all the other conditions were the same as those of Pd-Rh NTOs.

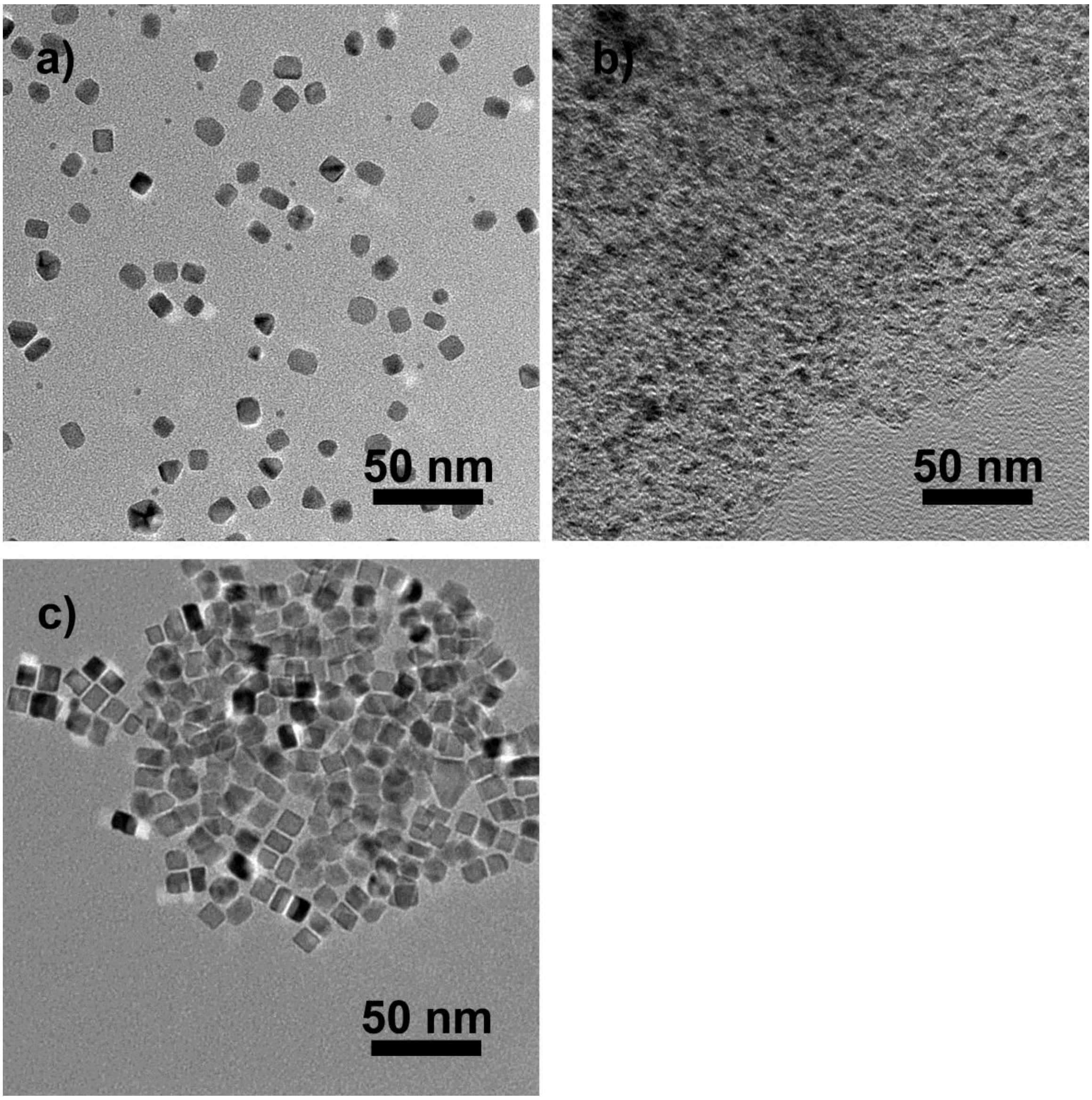

Figure S17. TEM image of a) Pd NCs synthesized under the similar conditions with those of Pd-Rh hollow NCs, b) commercial Pd/C, and c) Pd-Rh solid NCs synthesized under the similar conditions with those of Pd-Rh hollow NCs.

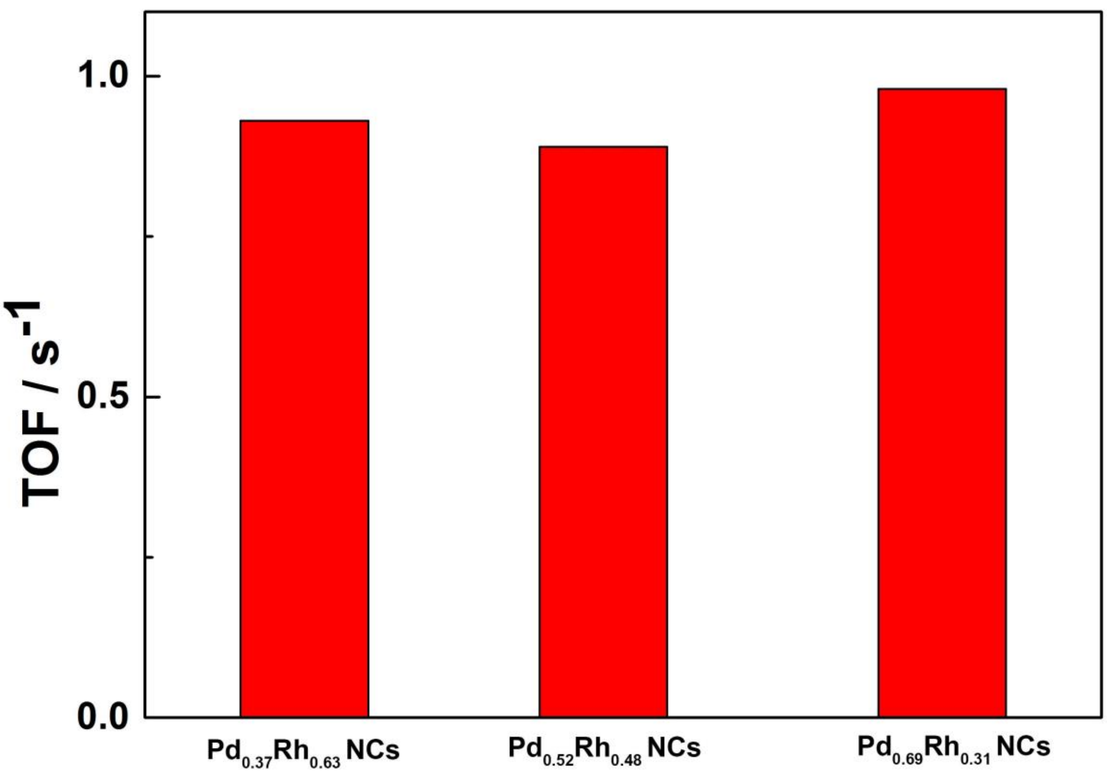

Figure S18. TOFs per surface Pd atom for Suzuki cross-coupling reaction with Pd-Rh solid NCs catalysts with various Pd/Rh ratios.

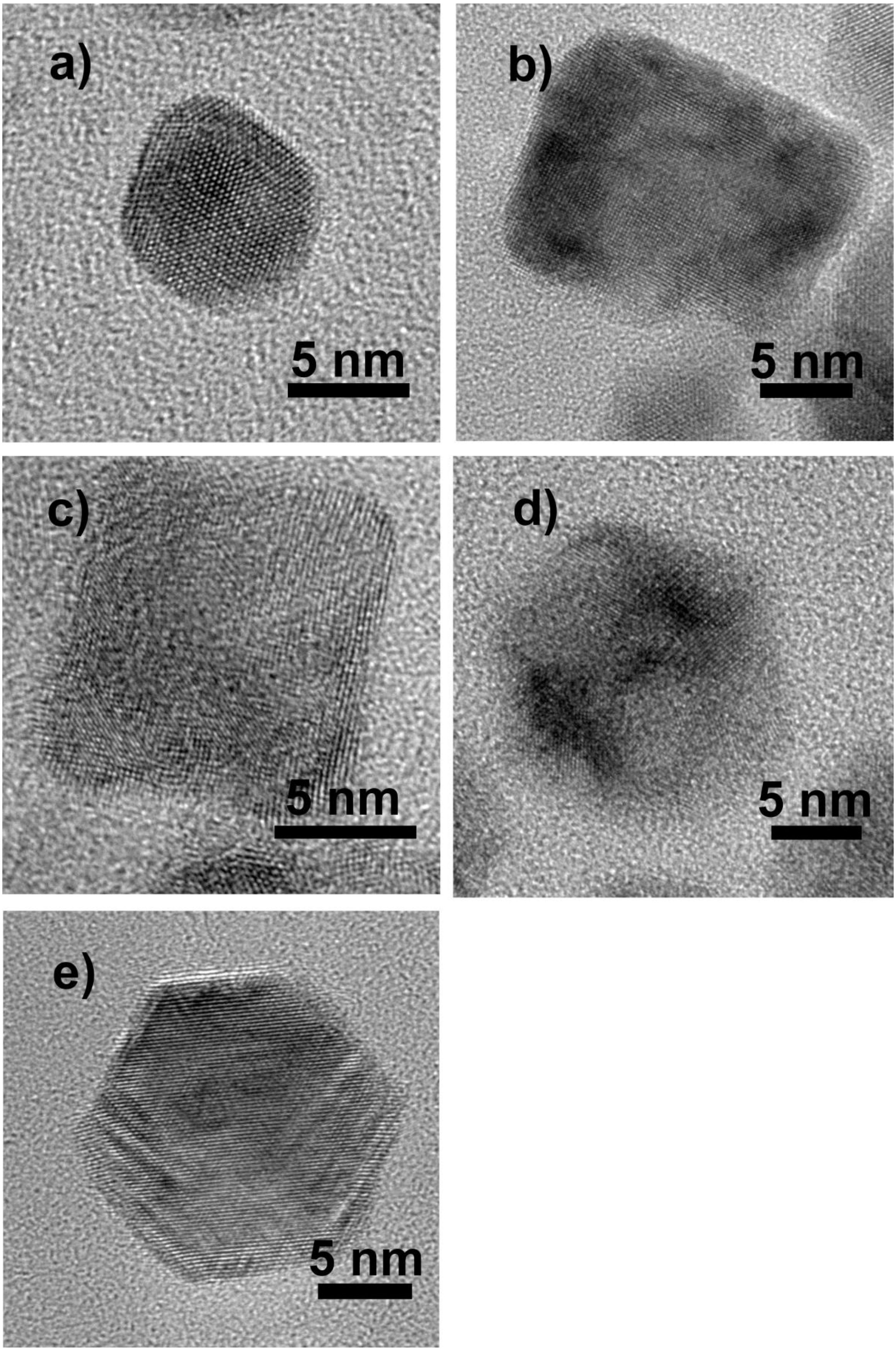

Figure S19. HRTEM images of nanocatalysts after Suzuki cross-coupling reactions: a) Pd NCs, b) Pd-Rh hollow NCs, c) Pd-Rh solid NCs, d) Pd-Rh NIs, and e) Pd-Rh NTOs.

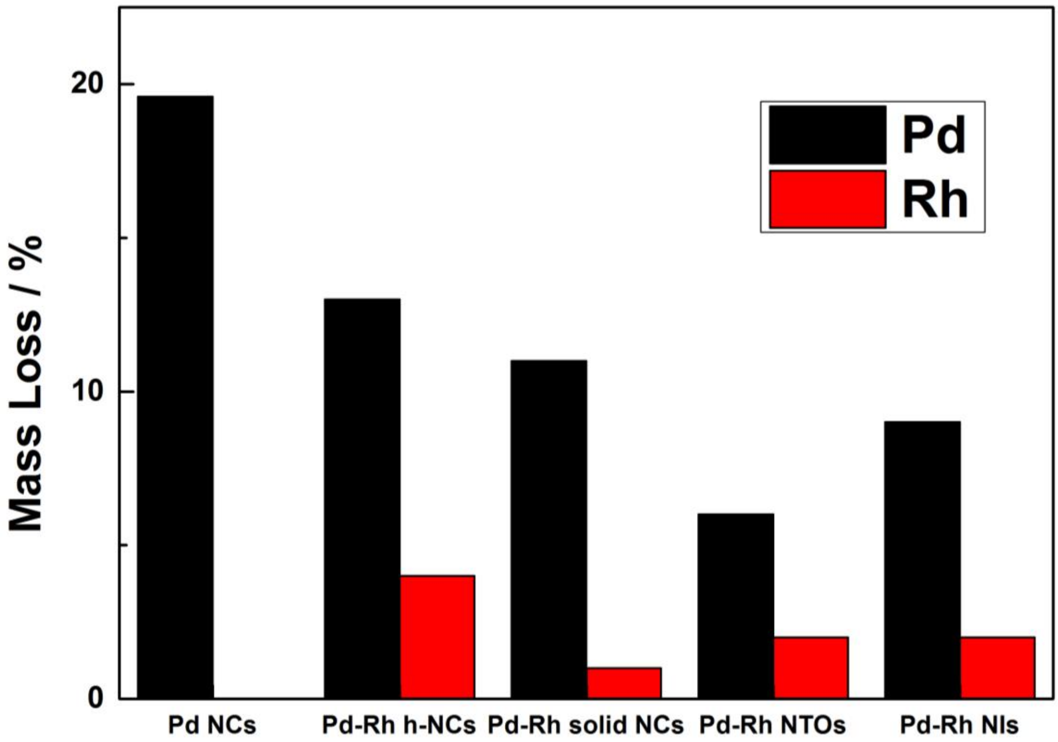

Figure S20. Mass loss of Pd and Rh in the as-tested nanocatalysts after Suzuki cross-coupling reactions (ICP-AES results).

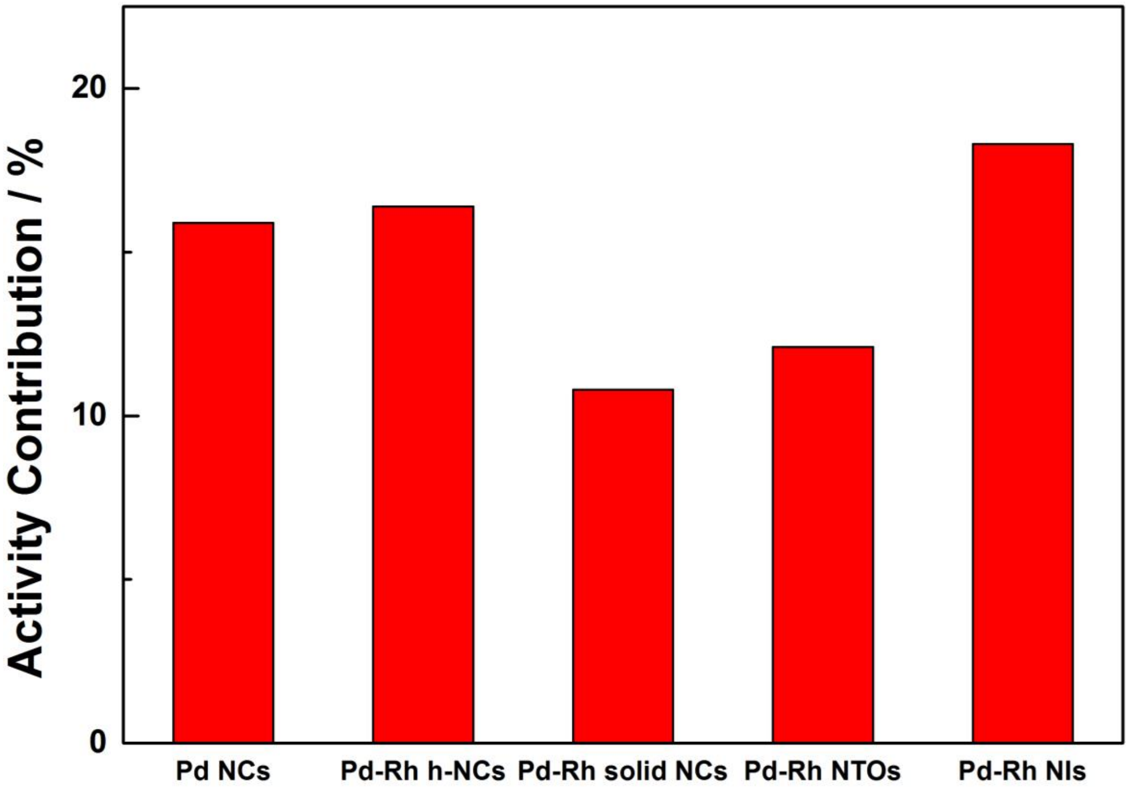

Figure S21. The contribution of the homogeneous Pd leached into solution to the overall catalytic activity of the nanocatalysts.